

# Development of a Method for Contactless Temperature Measurement in 3 Spectral Ranges

**Dimcho Pulov**

Department of Mechanical and Precision Engineering  
Technical University of Gabrovo  
Gabrovo, Bulgaria  
pulov@mail.bg

**Tsanko Karadzov**

Department of Mechanical and Precision Engineering  
Technical University of Gabrovo  
Gabrovo, Bulgaria  
karadzov\_s@abv.bg

**Abstract.** A 3-spectral method for non-contact temperature measurement has been developed. Three silicon photodiodes were used. The separation of the spectrum is done by optical bandpass filters and beamsplitters. It is possible to work in three modes: three-spectral, two-spectral (spectral ratio) and one-spectral. In the first mode, the temperature of objects with an unknown and variable emissivity can be measured. The last two modes give good results respectively for gray bodies and for objects with known emissivity.

**Keywords:** differential photo receiver, temperature, method, IR diaphragm, lens design.

## I. INTRODUCTION

Temperature is one of the main parameters that determine the state of substance. The efficient functioning of a large number of technological processes in the industry is related to maintaining the temperature within certain limits and with a specified accuracy. For this reason, accurate temperature measurement is essential to modern science and technology.

Remote methods of temperature measurement are increasingly used. These are optical methods that are based on the registration of the own thermal radiation of the investigated objects in the infrared spectrum [1]–[4]. Regardless of their advantages, optical pyrometers have one serious drawback which necessarily must be accounted for. All non-contact measurements are based on Planck's law, which relates the spectral radiant exitance of a black body  $M_{bb}(\lambda, T)$ , its temperature  $T$  and the wavelength  $\lambda$ .

$$M_{bb}(\lambda, T) = \frac{C_1}{\lambda^5 \left[ \exp\left(\frac{C_2}{\lambda T}\right) - 1 \right]} \quad (1)$$

The real objects whose temperature is measured are not black and therefore it can be recorded

$$M(\lambda, T) = M_{bb}(\lambda, T) \varepsilon(\lambda, T)$$

where  $\varepsilon(\lambda, T)$  is the emissivity.

The emissivity of real bodies varies from 0 for an ideal mirror to 1 for a black body. If  $\varepsilon(\lambda, T) = \text{const.}$ , the body is called gray.

Therefore, the pyrometer output signal depends simultaneously on two unknown quantities: the actual temperature of the object  $T_{obj}$  (which is to be measured) and its emissivity  $\varepsilon(\lambda, T)$ .

This implies an indeterminacy of the results of the measurements and the appearance of a difference  $\Delta T$  between the actual temperature of the object  $T_{obj}$  and the measured one  $T_{meas}$  ( $T_{meas} = T_{obj} - \Delta T$ ).

Several types of pyrometers are known:

- Radiation pyrometers. The measured value is equal to the temperature of a black body at which its radiance is equal to the radiance of the object under study. For them

$$T_{obj} = \frac{T_{meas}}{\sqrt[4]{\varepsilon(T)}} \quad \text{или} \quad \frac{\Delta T}{T} = 1 - \sqrt[4]{\varepsilon(T)}$$

where  $\varepsilon(T)$  is the integral emissivity in the working spectral range of the device  $\Delta\lambda$ .

Radiation pyrometers correctly measure temperatures only of black bodies or of bodies with a known emissivity  $\varepsilon(T)$ .

Print ISSN 1691-5402

Online ISSN 2256-070X

<https://doi.org/10.17770/etr2023vol3.7184>

© 2023 Dimcho Pulov, Tsanko Karadzov. Published by Rezekne Academy of Technologies.  
This is an open access article under the [Creative Commons Attribution 4.0 International License](https://creativecommons.org/licenses/by/4.0/).

- Spectral ratio pyrometers. The measured temperature  $T_{meas}$  is numerically equal to the blackbody temperature, where the ratio of the spectral radiant exitance  $M(\lambda, T)$  for two narrow spectral ranges is equal to the same ratio, but for the controlled object at its actual temperature  $T_{obj}$ . The spectral ratio pyrometers correctly measure the temperature of only gray bodies or bodies with a known  $\varepsilon_1/\varepsilon_2$  ratio [5], [6], because for them

$$\frac{1}{T_{obj}} - \frac{1}{T_{meas}} = \frac{\lambda_1 \lambda_2}{C_2(\lambda_2 - \lambda_1)} \cdot \ln\left(\frac{\varepsilon_1}{\varepsilon_2}\right) \quad (2)$$

- Spectral pyrometers. Temperature is measured by registration the radiation spectrum of the object and comparing it to the spectrum of a black body. Receiving information in many channels allows correction of the unknown emissivity [7],[8] and temperature measurement of non-gray bodies for which  $\varepsilon = f(\lambda)$ .

In this method, the separation of the spectrum is realized by using spectrometers with diffraction gratings [9], which are expensive devices. In addition, the presence of many spectral channels implies the acquisition of large data sets, as well as complex algorithms and mathematical expressions for determining the true temperature [10] – [13].

As a compromise option, an improvement of the two-wave spectral ratio pyrometer can be proposed by adding one more spectral channel. In this way, additional information about the emissivity will be obtained, which will reduce the error of measurements caused by its unknown.

The aim of the given publication is the development of a pyrometer operating in 3 narrow spectral ranges, which allows temperature measurement of non-gray bodies and the separation of the spectral channels is realized by simple beamsplitters.

## II. EXPOSITION

### A. Essence of the three-spectral method

The three-spectral method is a development and improvement of the two-spectral pyrometric method. It measures the radiant exitance in 3 narrow spectral intervals  $\Delta\lambda_i$  using 3 photodiodes. The centers of these intervals  $\lambda_i$  are respectively  $\lambda_1, \lambda_2$  и  $\lambda_3$ , for which the ratio  $\lambda_1 < \lambda_2 < \lambda_3$  applies. The approximation of the unknown emissivity with a suitable function adequately characterizing the dependence  $\varepsilon = f(\lambda, T)$  is the basis of the three-spectral method.

The signal at the output of the photo receiver in the spectral interval  $i$  is defined as

$$I_i(T) = Ad\Omega \int_{\Delta\lambda_i} M(\lambda)S(\lambda)\tau(\lambda)d\lambda \quad (3)$$

where:  $A$  – area of the entrance pupil of the optical system;  $\Omega$  – solid angle of the field of view;  $M(\lambda)$  – spectral radiant exitance of the measured body;  $S(\lambda)$  – spectral sensitivity of the photo receiver;  $\tau(\lambda)$  – transmittance of the all optical components (lens, beam splitter, filter, medium).

It can be assumed that in narrow parts of the spectrum, the spectral sensitivity of the photo receiver and the transmittance of the optical system do not change. Furthermore, when the measured body is located relatively close to the pyrometer, the transmittance of the medium can be neglected. Then expression (3) takes the form

$$I_i(T) = K_i \varepsilon_i(\lambda) M_{bbi}(\lambda) \quad (4)$$

where  $K_i$  is a constant depending on the summary characteristics of the pyrometer;  $M_{bbi}(\lambda)$  – spectral radiant exitance of a black body.

Using the Vin approximation for the short-wavelength region of the spectrum, expression (4) takes the form

$$I_i(T) = K_i \varepsilon_i(\lambda) \frac{C_1}{\lambda_i^5 \exp\left(\frac{C_2}{\lambda_i T}\right)} \quad (5)$$

It can be assumed that for narrow and closely spaced spectral sections, the pyrometer constant does not change, i.e.  $K_i = const$ . When measuring in two spectral ranges ( $i = 1, 2$ ) and from expression (5), the ratio  $I_1(T)/I_2(T)$  is expressed.

After its two-sided logarithm the temperature of the object is determined as

$$T = \frac{C_2 \left(1/\lambda_2 - 1/\lambda_1\right)}{\ln\left(\frac{I_1(T)}{I_2(T)} \cdot \frac{\lambda_1^5}{\lambda_2^5}\right)} \quad (6)$$

When measuring in 3 spectral ranges ( $i = 1, 2, 3$ ), expression (5) is converted into a system of 3 equations with 4 unknowns ( $\varepsilon_1(\lambda), \varepsilon_2(\lambda), \varepsilon_3(\lambda)$  and  $T$ ).

$$\begin{cases} I_1(T) = \varepsilon_1(\lambda) \lambda_1^{-5} \exp\left(-\frac{C_2}{\lambda_1 T}\right) \\ I_2(T) = \varepsilon_2(\lambda) \lambda_2^{-5} \exp\left(-\frac{C_2}{\lambda_2 T}\right) \\ I_3(T) = \varepsilon_3(\lambda) \lambda_3^{-5} \exp\left(-\frac{C_2}{\lambda_3 T}\right) \end{cases}$$

This system is undefined. In order for it to be solved correctly, it is necessary to introduce another equation connecting these unknown quantities. Determining the true (thermodynamic) temperature of non-gray bodies under such indeterminacy involves using a priori assumptions about the form of the function  $\varepsilon = f(\lambda, T)$ . This means modeling the behavior of the emissivity based on substantiated theoretical and experimental data. The spectral emissivities of various metals are shown in fig. 1.

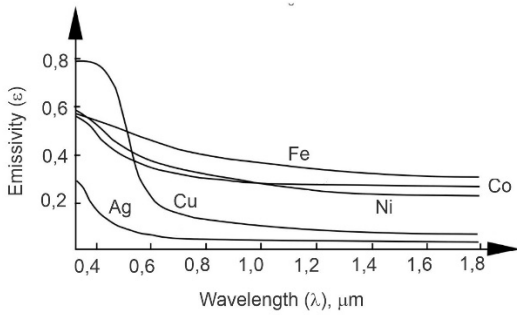


Fig. 1. Spectral emissivity of various metals.

It is shown in [14]–[17] that various approximation functions are possible, but the exponential is the most used because of the convenient mathematical operations with it. In [11],[12] various exponential functions are investigated and it is found that the emissivity of many metals is successfully approximated by an exponential function of the form

$$\varepsilon(\lambda, T) = \varepsilon_0(T) \exp(a\lambda) \quad (7)$$

where  $\varepsilon_0(T)$  is the dependence of the emissivity on temperature.

Considering expression (7) the signal at the output of the photo receiver can be written as

$$I_i(T) = \varepsilon_0(T) \exp(a\lambda) \frac{C_1}{\lambda_i^5 \exp\left(\frac{C_2}{\lambda_i T}\right)} \quad (8)$$

After logarithmizing both sides of expression (8) for the three spectral ranges ( $i = 1, 2, 3$ ), the following system of equations is obtained

$$\begin{cases} \ln(I_1) = \ln(\varepsilon_0(T)) + a\lambda_1 + \ln(C_1) - 5\ln(\lambda_1) - \frac{C_2}{\lambda_1 T} \\ \ln(I_2) = \ln(\varepsilon_0(T)) + a\lambda_2 + \ln(C_1) - 5\ln(\lambda_2) - \frac{C_2}{\lambda_2 T} \\ \ln(I_3) = \ln(\varepsilon_0(T)) + a\lambda_3 + \ln(C_1) - 5\ln(\lambda_3) - \frac{C_2}{\lambda_3 T} \end{cases}$$

This is a definite system of 3 equations with 3 unknowns ( $\varepsilon_0(T)$ ,  $a$  and  $T$ ). Its solution gives the value of the measured non-gray body temperature as a function of the measured signals at the output of the three photo receivers

$$T = \frac{C_2}{\lambda_1 \lambda_2 \lambda_3 (A + B)} \quad (9)$$

where the coefficients  $A$  and  $B$  are:

$$A = \frac{\ln\left(\frac{I_1}{I_3} \cdot \frac{\lambda_1^5}{\lambda_3^5}\right)}{(\lambda_3 - \lambda_2)(\lambda_3 - \lambda_1)} \quad B = \frac{\ln\left(\frac{I_1}{I_2} \cdot \frac{\lambda_1^5}{\lambda_2^5}\right)}{(\lambda_3 - \lambda_2)(\lambda_1 - \lambda_2)}$$

### B. Development of a block functional diagram of a three-spectral pyrometer.

In fig.2 shows the functional diagram of the developed three-spectral pyrometer. The heated object emits a flux in a hemisphere. Part of the flux falls on the objective of the pyrometer and is collected on the beamsplitter.

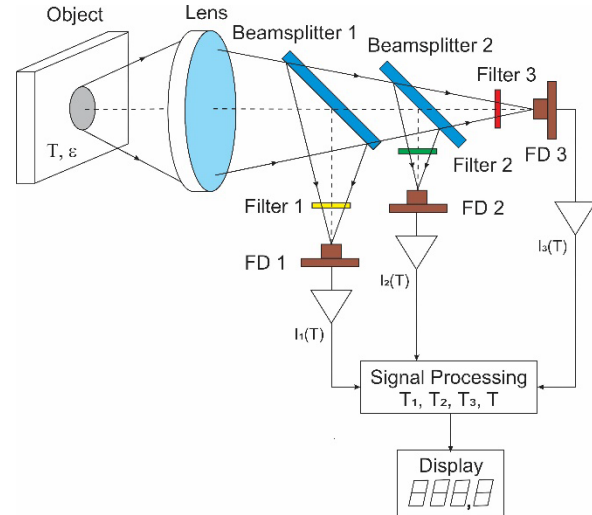


Fig. 2. Functional diagram of three-spectral pyrometer.

Three identical beamsplitters are provided in the scheme, which partially transmit and partially reflect the optical flow. The light dividers direct the radiation to three identical silicon photodiodes. Before the photo receivers, there are bandpass filters that limit the width of the spectral ranges. The parameters of the elements used in the pyrometer are shown in Table 1.

TABLE 1 THE PARAMETERS OF THE ELEMENTS USED IN THE THREE-SPECTRAL PYROMETER

	Spectral Band		
<b>Number</b>	1	2	3
<b><math>\Delta\lambda_i</math></b>	775-825nm	825-875nm	875-925nm
<b>Lens</b>	Achromatic Doublet AC254-100-B-ML - Thorlabs catalog		
<b>Beamsplitters</b>	BSW11 from Thorlabs catalog		
<b>Filters</b>	Bandpass Filters from Edmund Optics		
<b>Number</b>	# 84-789	#84-790 850	# 84-791
<b>CWL, <math>\lambda_i</math></b>	800 nm	nm	900 nm
<b>FWHM</b>	50 nm	50 nm	50 nm
<b>Photo Receivers</b>	Silicone Photodiodes Hamamatsu S2386		

### C. Schematic electrical diagram of the device

In fig.3 is shown the principle electrical circuit of device. Silicon photodiodes were used as photodetectors. Photodiodes produce electrical signals proportional to optical flow. The photocurrent  $I_{ph}$  through the photodiodes

is converted to voltage using operational amplifiers with feedback LM358.

In the block for electronic processing, these signals are amplified, their ratio is determined, which is subsequently converted into a value of the measured temperature of the controlled object.

An 8-bit microcontroller PIC18F252 is used to control the operation of the device, which has a 10-bit analog-to-digital converter. The controller has enough input-output ports and a sufficient amount of program memory in which the control program can be located.

Threshold voltages that determine the measuring range of the converter are respectively  $V_{REF-} = 0\text{ V}$  and  $V_{REF+} = 5\text{ V}$

V. The analog input signal to the ADC is represented by  $2^{10}$  or 1024 levels. The voltage increase step is determined by the formula:

$$\Delta U = \frac{V_{REF+}}{2^{10}} = \frac{5}{1024} = 4,883\text{ mV}$$

The functional scheme of the device is composed of three measuring channels. The voltage from the outputs of the current-voltage converters is fed to three analog inputs of the controller RA1/AN1, RA2/AN2 and RA3/AN3. The analog-to-digital converter is one and the inputs are switched. Only one input voltage is measured at any given time.

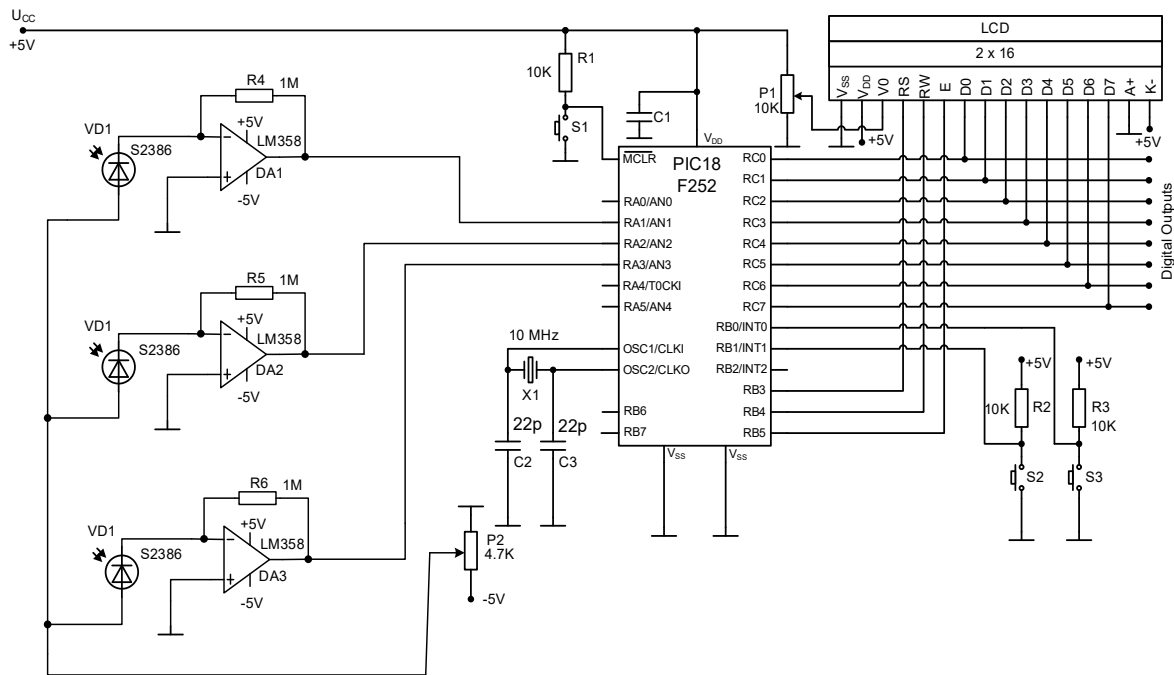


Fig. 3. Basic circuit diagram.

#### D. Block chart of the algorithm of the program

The block diagram of the control program algorithm is shown in fig. 4. At the beginning, the controller is initialized, constants and variables are defined, saving corresponding cells from the data memory for them. Next, it is determined which I/O ports will be used. Set which microcontroller pins to be digital inputs, analog inputs and digital outputs. The display is then initialized. The main program is a continuous loop that only breaks when the analog-to-digital converter has finished measuring the voltage. The processing of the result of each measurement takes place in a subroutine, which is started when an interruption occurs from the analog-to-digital converter.

#### E. Connecting the LCD to the microcontroller

At the beginning of the subroutine, the analog input for the next measurement is selected. After that, the result of the previous measurement is processed, which includes – hardware multiplication of the value of the measurement with a preset constant. The measured voltages from the three channels are compared. The result is converted from

hexadecimal to binary-decimal code. After that, the results of the measurements are displayed on the LCD display. First, the output addresses are determined, which means at which position each digit of the result should be displayed. The calculated values are then visualized. Finally, the subroutine starts the next measurement and returns to the main program.

A two-line alphanumeric LCD display is used, and 16 characters can be displayed on each line. To control the LCD module, a control bus is used, including pins RS, R/W, E, which are connected respectively to pins RB3, RB4, RB5 of the microcontroller initialized as digital outputs. The display data bus consists of 8 pins. With their help, the microcontroller communicates with the LCD module. Display pins D0, D1, D2, D3, D4, D5, D6 and D7 are initialized as inputs and are connected respectively to microcontroller pins RC0, RC1, RC2, RC3, RC4, RC5, RC6 and RC7 which are initialized as exits. At the beginning of the program, the display is also initialized.

Finally, the measured values are displayed on the display, and the user could choose different operating

modes of the device. The operation mode of the measuring system is mainly determined by the operation mode of the microcontroller, which is set by entering certain values in the registers defining the special functions. For a given measurement, the photodiodes can be used separately, and the result measured with each photodiode can be compared, or they can be used together, and a total result can be obtained.

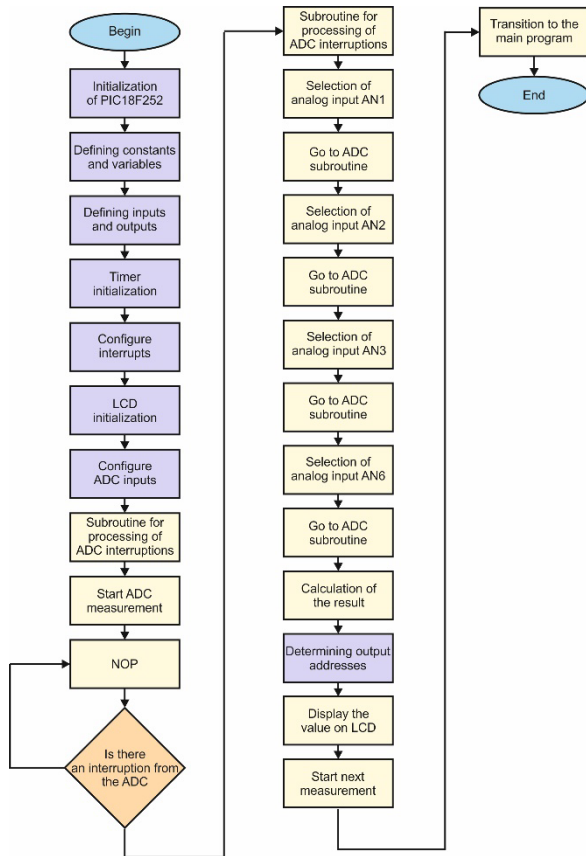


Fig. 4. Block chart of the algorithm of the program.

#### F. Algorithm for the operation of a device

The pyrometer operation algorithm can be presented with the following sequence.

1. The signals at the outputs of the three photodiodes are measured  $I_1(T)$ ,  $I_2(T)$  и  $I_3(T)$ .
2. According to expression (6), the ratio temperatures are calculated for the combinations containing two spectral ranges respectively

$$T_1 = T(\Delta\lambda_1, \Delta\lambda_2) = f\left(\frac{I_1}{I_2}\right)$$

$$T_2 = T(\Delta\lambda_2, \Delta\lambda_3) = f\left(\frac{I_2}{I_3}\right)$$

$$T_3 = T(\Delta\lambda_1, \Delta\lambda_3) = f\left(\frac{I_1}{I_3}\right)$$

3. It is checked whether the body is gray. It will be grayed out if  $T_1 = T_2$ . This equality is not strictly enforced in the general case. Nevertheless, the measured body can be assumed to be gray if the condition is met

$$T_1 = T_2 \pm \delta T \quad (10)$$

where  $\delta T$  is the permissible measurement error. If condition (10) holds, then the temperature of body is defined as

$$T = \frac{\sum_{i=1}^3 T_i}{3}$$

4. If condition (10) is not fulfilled, then the temperature of body is determined by expression (9).

The total error of the proposed three-spectral pyrometer is determined by the instrumental error, the blackbody pyrometer calibration error, the error due to the presence of parasitic reflections, the error due to the background radiation from near spaced high-temperature sources falling into the field of view of the device, and the methodological error caused by the approximation error of the emissivity [18],[19]. When measuring the temperature of highly heated metals ( $800 \div 2000$ )°C, the methodological error has the greatest influence. In the indicated temperature range, for many metals, an exponential dependence of  $\varepsilon = f(\lambda, T)$ . The use of narrow and close spectral intervals together with the exponential approximation of the emissivity leads to a small methodological error, which, depending on the temperature of the body and the width of the spectral interval, varies from 0,5% to 1%.

### III. CONCLUSION

A three-spectral pyrometer using three narrow spectral regions has been developed. Under substantiate assumptions about  $\varepsilon(\lambda, T) = const.$  temperature is determined as the average of three ratio temperatures for three wavelength pairs. In the most general case, a three-wave method is implemented by modeling the emissivity using an exponential function. The use of narrow and close spectral intervals in totality with the exponential approximation of the emissivity leads to a reduction of the uncertainty in the measurement of the temperature of non-gray bodies with an unknown dependence  $\varepsilon(\lambda, T)$ .

### REFERENCES

- [1] Z. M. Zhang, B. Tsai and G. Machin. Radiometric temperature measurements, Berlin: Elsevier, 2009.
- [2] V. Vavilov and D. Burleigh, Infrared Thermography and Thermal Nondestructive Testing, Springer International Publishing: New York, NY, USA, 2020.
- [3] K. Grujić, "A Review of Thermal Spectral Imaging Methods for Monitoring High-Temperature Molten Material Streams", Sensors, Vol. 23, Issue 3, Febr. 2023, doi: 10.3390/s23031130.
- [4] M.A. Khan, C. Allemand and T.W. Eagar, "Noncontact temperature measurement. I Interpolation based techniques", Review of Scientific Instruments, Vol. 62, Issue 2, pp. 392 – 402, 1991, doi: 10.1063/1.1142133.
- [5] T. Fu, X. Cheng and X. Yang, "Theoretical evaluation of measurement uncertainties of two-color pyrometry applied to optical diagnostics", Applied Optics, Vol. 47, Issue 32, pp. 6112 – 6123, Nov. 2008, doi: 10.1364/AO.47.006112.
- [6] B.K. Tsai, R.L. Shoemaker, D.P. DeWitt, B.A. Cowans, Z. Dardas, W.N. Delgass and G. J. Dail, "Dual-wavelength radiation thermometry: emissivity compensation algorithms", International

- Journal of Thermophysics, Vol. 11, Issue 1, pp. 269 – 281, Jan. 1990, doi: 10.1007/BF00503877.
- [7] P.B. Coates, “Multi-wavelength pyrometry”, *Metrologia*, Vol. 17, Issue 3, pp. 103 – 109, 1981, doi: 10.1088/0026-1394/17/3/006.
- [8] A. Araújo, “Analysis of multi-band pyrometry for emissivity and temperature measurements of gray surfaces at ambient temperature”, *Infrared Physics and Technology*, Vol. 76, pp. 365 – 374, May 2016, doi: 10.1016/j.infrared.2016.03.014.
- [9] W. Wójcik, V. Firago, A. Smolarz, I. Shedreyeva and B. Yeraliyeva, “Multispectral High Temperature Thermography”, *Sensors* 2022, 22, 742, doi: 10.3390/s22030742.
- [10] T. Fu, X. Cheng, X. Fan and J. Ding, “The analysis of optimization criteria for multi-band pyrometry”, *Metrologia*, Vol. 41, Issue 4, pp. 305 – 313, August 2004, doi: 10.1088/0026-1394/41/4/012.
- [11] V. Firago and W. Wojcik, “High-temperature three-colour thermal imager”, *Przeład Elektrotechniczny*, Vol. 91, Issue 2, pp. 208–214, 2015, doi: 10.15199/48.2015.02.47.
- [12] H. Madura, M. Kastek and T. Piatkowski, “Automatic compensation of emissivity in three-wavelength pyrometers”, *Infrared Physics and Technology*, Vol. 51, Issue 1, pp. 1 – 8, July 2007, doi: 10.1016/j.infrared.2006.11.001.
- [13] P. Saunders, “Reflection errors and uncertainties for dual and multiwavelength pyrometers”, *High Temperatures - High Pressures*, Vol. 32, Issue 2, pp. 239 – 249, 2000, doi: 10.1068/htrt201.
- [14] A. Sala, *Radiant Properties of Materials*, PWN & Elsevier, 1986.
- [15] D. P. DeWitt and J. C. Richmond, “Thermal radiative properties of materials,” in *Theory and practice of radiation thermometry*, 1988, pp. 171–175.
- [16] D.Y. Svet, Determination of the emissivity of a substance from the spectrum of its thermal radiation and optimal methods of optical pyrometry, *High Temp. – High Press.*, Vol. 8, Issue 5, pp. 493 – 498, 1976.
- [17] T. Hartsfield, A. Iverson and J. Baldwin, “Reflectance determination of optical spectral emissivity of metal surfaces at ambient conditions,” *Journal of Applied Physics*, Vol.124, Issue 10, Sept. 2018, doi: 10.1063/1.5042601.
- [18] M.J. Marinov, B.I. Stoychev, D.M. Guteva and M.V. Georgiev, “Computer modeling and geometric analysis of Click-Clack mechanisms”, *Journal of Mechanics of Machines*, vol. 118, pp.35-39, 2016.
- [19] Dichev, D., F. Kogia, H. Nikolova, D. Diakov. A Mathematical Model of the Error of Measuring Instruments for Investigating the Dynamic Characteristics. *Journal of Engineering Science and Technology Review*. Volume 11, Issue 6, 2018, pp. 14-19, doi: 10.25103/jestr.116.03.